

See discussions, stats, and author profiles for this publication at: <https://www.researchgate.net/publication/236023566>

# Fourier Transform Fluorescence and Phosphorescence of Porphine in Rare Gas Matrices

ARTICLE *in* THE JOURNAL OF PHYSICAL CHEMISTRY · JANUARY 1991

Impact Factor: 2.78

---

CITATIONS

22

---

READS

8

4 AUTHORS, INCLUDING:



J. Waluk

Polish Academy of Sciences

257 PUBLICATIONS 3,706 CITATIONS

SEE PROFILE

cerning the free energy surface of CIP and its intersection with ground-state surface as well as the mechanism of CR decay of the CIP might be obtained by examining the temperature effects on  $k_{CR}^{CIP}$  of various D,A systems, which are now going on in this laboratory.

(c) We have also examined the dissociation processes of the IP's into free ions for several weak D,A systems. In the case of the excitation of the CT complex with strong D,A systems, the CIP state undergoes very fast CR deactivation leading to practically zero dissociation yield. Our results of the direct observation of the dissociation process did not give any positive support for the conventional mechanism assuming SSIP as a definite intermediate state in the dissociation from CIP to free ions. From the

present results as well as our previous results<sup>16,17</sup> of the direct observation on the ionic dissociation processes from the excited CT complexes, it can be concluded that the example of the photoinduced ionic dissociation of CT complexes by the two-step mechanism including single type SSIP,  $CIP \rightarrow SSIP \rightarrow$  free ions, is very limited, and actually, many systems seem to undergo gradual change of structure from the excited CT complex to CIP and then to free ions probably via several intermediate states of loose structure SSIP's (LIP).

**Acknowledgment.** N.M. acknowledges the support by a Grant-in-Aid (No. 62065006) from the Ministry of Education, Science and Culture, Japan.

## Fourier Transform Fluorescence and Phosphorescence of Porphine in Rare Gas Matrices

Juliusz G. Radziszewski,\* Jacek Waluk,<sup>1a</sup> Miloš Nepraš,<sup>1b</sup> and Josef Michl\*

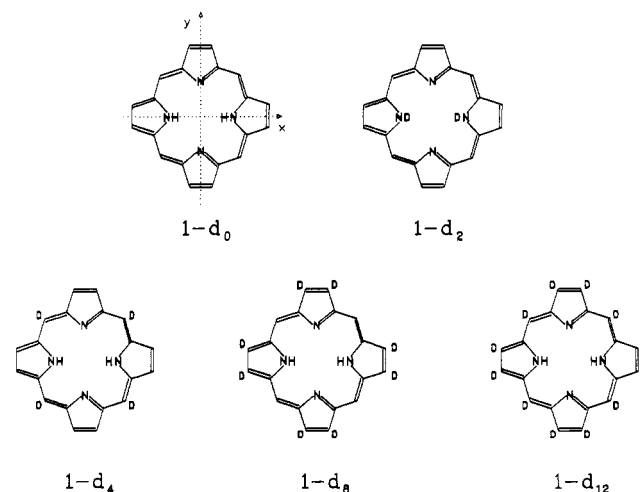
Center for Structure and Reactivity, Department of Chemistry and Biochemistry, The University of Texas at Austin, Austin, Texas 78712-1167 (Received: June 13, 1990; In Final Form: September 17, 1990)

Matrix-isolated free-base porphine and its deuterated analogues show highly resolved intense fluorescence in neon, with evidence of strong  $b_{1g}$  vibronic activity, and highly resolved intense phosphorescence in xenon, dominated by totally symmetric vibrations. Triplet lifetimes were determined from T-T absorption decay, which revealed a new band at 310 nm. It was concluded that the heavy-atom enhancement of the  $T_1 \rightarrow S_0$  radiative rate is dramatic. Both emissions exhibit site structure, and single-site spectra were obtained upon narrow-bandwidth excitation. The  $T_1 \rightarrow S_0$  emission site pattern is identical with that of  $S_1 \rightarrow S_0$  emission and  $S_1 \leftarrow S_0$  absorption and totally different from that of  $S_2 \leftarrow S_0$  absorption, suggesting that  $T_1$  and  $S_1$  are both  $Q_x$  and have a common orbital origin, contrary to the currently accepted assignment. The implications of the results for the mechanism of the photoinduced double proton transfer in free-base porphine are considered. All the results are compatible with the proposal that the isomerization occurs in  $T_1$  in a stepwise fashion through the "cis" isomer. The advantages of interferometric recording of highly resolved visible and near-IR emission spectra are pointed out.

Although the porphyrins have long been a fashionable object to study in organic spectroscopy, some important issues still remain to be clarified for the parent compound of the series, free-base porphine (1). For example, (i) no highly resolved phosphorescence has been reported so far, and the intensity of the reported low-resolution phosphorescence spectra<sup>2,3</sup> was too weak to permit an analysis of vibronic structure, (ii) the assignment of the symmetry of the lowest triplet state has only been made indirectly, on the basis of comparison of ESR spectra with the results of simple MO calculations,<sup>4</sup> and (iii) the mechanism of the photoinduced double proton transfer observed for porphine and its derivatives<sup>5-9</sup> has not been elucidated. It is not clear whether the protons move stepwise or synchronously, whether this process occurs in the excited singlet or triplet state or both, or whether it is a hot ground-state reaction.

In the present work, we report highly resolved fluorescence and phosphorescence of free-base porphine ( $1-d_0$ ) and its deuterated

CHART I



derivatives  $1-d_2$ ,  $1-d_4$ ,  $1-d_8$ , and  $1-d_{12}$  (Chart I) in noble gas matrices. In previous papers, we discussed the merits of using rigid rare gas solvents for the determination of transition polarizations in the IR<sup>10</sup> and visible<sup>11</sup> absorption regions. This was accomplished by Fourier transform (FT) measurements on photooriented<sup>12,13</sup> samples. Presently, we use the FT technique to

(1) (a) Permanent address: Institute of Physical Chemistry, Polish Academy of Sciences, 01-224, Warsaw, Kasprzaka 44, Poland. (b) Permanent address: Research Institute of Organic Syntheses, 532 18 Pardubice-Rybitvi, Rybalkova 1361, Czechoslovakia.

(2) Gouterman, M.; Khalil, G.-E. *J. Mol. Spectrosc.* **1974**, *53*, 88.

(3) Tsvirko, M. P.; Solov'ov, K. N.; Gradyushko, A. T.; Dvornikov, S. S. *Opt. Spectrosc. (Engl. Transl.)* **1975**, *38*, 400.

(4) Van Dorp, W. G.; Soma, M.; Kooter, J. A.; van der Waals, J. H. *Mol. Phys.* **1974**, *28*, 1551.

(5) Zaleski, I. E.; Kotlo, V. N.; Sevchenko, A. N.; Solov'ev, K. N.; Shkirman, S. F. *Sov. Phys.—Dokl. (Engl. Transl.)* **1973**, *17*, 1183.

(6) Solov'ev, K. N.; Zaleski, I. E.; Kotlo, V. N.; Shkirman, S. F. *Phys. Lett.* **1973**, *17*, 332.

(7) Korotaev, O. N.; Personov, R. I. *Opt. Spectrosc. (Engl. Transl.)* **1972**, *32*, 479.

(8) Völker, S.; van der Waals, J. H. *Mol. Phys.* **1976**, *32*, 1703.

(9) Voelker, S.; Macfarlane, R. M.; Genack, A. Z.; Trommsdorff, H. P.; van der Waals, J. H. *J. Chem. Phys.* **1977**, *67*, 1759.

(10) Radziszewski, J. G.; Waluk, J.; Michl, J. *Chem. Phys.* **1989**, *136*, 165.

(11) Radziszewski, J. G.; Waluk, J.; Michl, J. *J. Mol. Spectrosc.* **1990**, *140*, 373. In this paper, the graphics of Figures 6 and 10 were interchanged in the publication process, and the graphics of Figure 4 are not shown at all (this figure contains a repeat of the graphics of Figure 9). The captions of all the figures refer correctly to the originally intended graphics.

investigate the emission spectra, taking advantage of its high resolution, speed, and, in particular, very high sensitivity in the near-IR region, which is a difficult region to access by conventional luminescence spectrometers. Moreover, we find that the use of Xe as a matrix greatly enhances phosphorescence intensity, presumably by an external heavy-atom effect that increases the triplet to ground-state radiative rate. Triplet lifetimes were obtained by measurements of transient triplet-triplet absorption by flash photolysis.

The paper is organized as follows: First, we present luminescence spectra in different matrices and show the site structure and ground-state vibrational energies and symmetries obtained from the analysis of vibronic structure of fluorescence and phosphorescence. Next, we analyze the resulting spectroscopic and photophysical information: (i) we provide evidence for a matrix effect upon the singlet and triplet excited-state depopulation rate constants, and (ii) we propose a reassignment of the orbital origin of the lowest triplet state. Then, we describe time-resolved triplet-triplet absorption spectra. Finally, we discuss the implications our results have for the elucidation of the mechanism of photoinduced double proton transfer in free-base porphine.

### Experimental Part

Free-base porphine ( $1-d_0$ ) was purchased from Porphyrin Products. Porphine- $d_2$  ( $1-d_2$ ), deuterated on the nitrogen atoms, was obtained by shaking a solution of  $1-d_0$  in  $CS_2$  with  $C_2H_5OD$ . Porphine- $d_4$  ( $1-d_4$ ), porphine- $d_8$  ( $1-d_8$ ), and porphine- $d_{12}$  ( $1-d_{12}$ ) were prepared from  $1-d_0$  according to literature procedures.<sup>14</sup> Isotopic purity of the deuterated porphines was checked by NMR and mass spectrometry.

All samples were prepared on close-cycle helium refrigerators. These were either a two-stage 10 K Displex (Air Products) or a three-stage 3.7 K Heliplex (APD Cryogenics). Low-temperature samples were prepared by sublimation of porphine at about 180 °C into a stream of noble gas (0.5–2 mL/min) and subsequent condensation on a sapphire or  $CaF_2$  cold window. The window temperature during the deposition was about 4 K for Ne matrices, 27 K for Ar, and 55 K for Xe matrices; this assures high optical quality of the matrix sample. During the measurements, samples were kept at about 4 or 10 K, depending on type of cryostat and noble gas used.

Absorption and emission spectra were recorded by using a Nicolet 60-SXR interferometer equipped with a quartz beam splitter and Si, Si-avalanche, and InGaAs detectors and band-pass filters removing unwanted higher energy radiation (in order to optimize the signal-to-noise ratio). High sensitivity of the Si-avalanche and InGaAs photodiodes, especially under very low light level conditions, and the large spectral range of the InGaAs element, which extends to 6500  $cm^{-1}$ , make these emission detectors preferable in the near-infrared region.

Absorption spectra were determined prior to emission measurements, using the same instrument.<sup>11</sup> In emission experiments, sample excitation at a desired wavelength was achieved by monochromatic light from a Coherent 600-21 CW ring dye laser (R6G) pumped with a Coherent Innova-100 Ar ion laser. All but a tiny fraction of the exciting light was blocked from reaching the detector. Exact frequency of the exciting light was then determined simultaneously with the emission spectrum by observing the peak due to the small fraction that entered, folded around the He-Ne laser frequency. Typical laser power on the sample was between 5 and 100 mW, loosely focused to a spot about 0.2–0.5 mm in diameter. The birefringent crystal in the ring laser was driven by a stepper motor controlled by pulses from the Nicolet interferometer computer, permitting us to scan the excitation wavelength in 0.2–0.5- $cm^{-1}$  steps and to record rapid

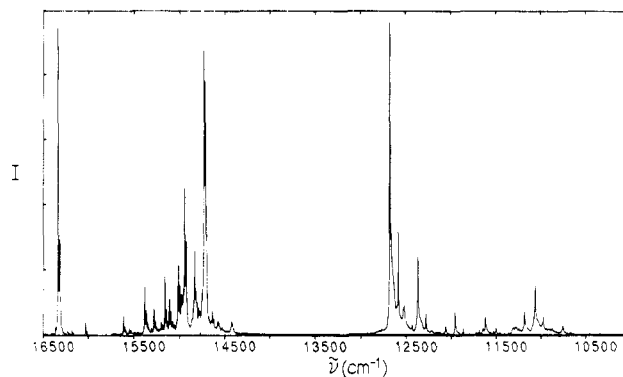


**Figure 1.** Luminescence of  $1-d_0$  in Ne (4 K) and Xe (10 K). The former is dominated by fluorescence (left) and the latter by phosphorescence (right).

spectra after each step. This allowed us to reduce to some extent the depletion of population of the site excited. This procedure offers an additional benefit, namely, access to excitation spectra, which are normally not easily available in FT luminescence work. These are obtained by careful photometric calibration of the instrument and by a precise measurement of the intensity of the exciting monochromatic light, step-scanning the exciting laser and recording a series of emission spectra.

The emitted light was collected at 180° geometry and collimated with a single plano-convex quartz lens of  $f/1.5$ , or  $f/4$  for polarization measurements. We have used resolution between 0.5 and 4  $cm^{-1}$ , and a typical measurement time was 5–30 s. In polarization experiments the sample was excited with polarized laser light, and the analyzing polarizer (FPI005 or FPI016, Melles Griot) was inserted into the collimated beam before the modulator, in parallel or perpendicular position with respect to the electric vector of exciting light.

Triplet lifetimes were determined by measuring the decays of T-T absorption intensities using a home-built transient absorption spectrometer. The sample was excited by the 308-nm line of an excimer laser (EMG 102, Lambda Physik, pulse duration  $\approx 10$  ns, pulse energy attenuated to 1–3 mJ). The probe pulse was provided by a xenon flash lamp (EG&G FX-200U flash tube plus a Lite Pac FY-604 trigger module). The delay between the pump and probe pulses was controlled by a CORDIN 437 digital time delay generator coupled with two programmable time delay modules (4141-1 Evans Electronics). For the detector part, we used a TN-6133 gated intensified photodiode array attached to the HR-320 (Instruments SA) spectrograph. The high-voltage signal for the intensifier (230 V, 10–1-ns duration) was provided by an AVTECH AVL-TN-1 pulse generator. Signals from the photodiode array were collected and averaged by a TN-1710 multichannel analyzer and processed by an IBM/PC microcomputer.

Fluorescence lifetimes were measured on a single photon counting instrument (PRA 510B flash lamp, Schoeffel GM 250 excitation and emission monochromators, RCA 1P28 photomultiplier, ORTEC 457 time-to-amplitude converter, TN-1213A analog-to-digital converter). The lifetimes were extracted from experimental decays by a deconvolution procedure based on a least-squares fitting algorithm.

### Results and Discussion

**Luminescence Spectra in Various Matrices.** Highly resolved fluorescence spectra of free-base porphine have been quite extensively studied in Shpolskii matrices<sup>15–26</sup> and anthracene crys-

(12) Radziszewski, J. G.; Burkhalter, F. A.; Michl, J. *J. Am. Chem. Soc.* **1987**, *109*, 61.

(13) Michl, J.; Thulstrup, E. W. *Spectroscopy with Polarized Light. Solute Alignment by Photoselection, in Liquid Crystals, Polymers, and Membranes*; VCH Publishers: Deerfield Beach, FL, 1986.

(14) Solov'ev, K. N.; Gladkov, L. L.; Gradyushko, A. T.; Ksenofontova, N. M.; Shulga, Z. M.; Starukhin, A. S. *J. Mol. Struct.* **1978**, *45*, 267.

(15) Gradyushko, A. T.; Solov'ev, K. N.; Starukhin, A. S. *Opt. Spectrosc. (Engl. Transl.)* **1976**, *40*, 267.

(16) Gradyushko, A. T.; Solov'ev, K. N.; Starukhin, A. S.; Shulga, A. M. *Opt. Spectrosc. (Engl. Transl.)* **1977**, *43*, 37.

(17) Bykovskaya, L. A.; Gradyushko, A. T.; Personov, R. I.; Romanovskii, Yu. V.; Solov'ev, K. N.; Starukhin, A. S.; Shul'ga, A. M. *Zh. Prikl. Spektrosk.* **1978**, *29*, 1088.

**TABLE I: Frequencies and Symmetries of Vibrations Observed in the Fluorescence Spectra of Porphine- $d_0$  in Ne at 4 K**

$\bar{\nu}$ , $\text{cm}^{-1}$		
site A <sub>1</sub> <sup>a</sup>	site B <sub>1</sub> <sup>b</sup>	symmetry <sup>c</sup>
104	105	b <sub>1g</sub>
155	153	a <sub>g</sub>
305	306	a <sub>g</sub>
608	610	(a <sub>g</sub> )
721	719	a <sub>g</sub>
786	784	b <sub>1g</sub>
874	873	
951	950	a <sub>g</sub>
972	971	b <sub>1g</sub>
990		a <sub>g</sub>
1001	999	
1027	1026	(a <sub>g</sub> )
1055	1054	a <sub>g</sub>
1103	1102	(b <sub>1g</sub> )
1134	1134	b <sub>1g</sub>
1175	1173	a <sub>g</sub>
1222	1220	b <sub>1g</sub>
1256	1257	
1278	1278	
	1301	(b <sub>1g</sub> )
1316	1315	b <sub>1g</sub>
1352	1350	a <sub>g</sub>
1360	1358	a <sub>g</sub>
	1365	a <sub>g</sub>
1379	1378	
1388	1387	b <sub>1g</sub>
1467		(a <sub>g</sub> )
1480		(a <sub>g</sub> )
1495	1494	a <sub>g</sub>
1502	1500	
1526	1526	
1575	1573	(b <sub>1g</sub> )
1578	1579	(b <sub>1g</sub> )
1600	1600	b <sub>1g</sub>
1612	1611	a <sub>g</sub>
1657	1657	(a <sub>g</sub> )
1693	1694	b <sub>1g</sub>
1752	1750	b <sub>1g</sub>
1801	1801	
1905	1906	b <sub>1g</sub>

<sup>a</sup> The lowest energy subsite of group A (16 309  $\text{cm}^{-1}$ ).<sup>11</sup> <sup>b</sup> The lowest energy subsite of group B (16 322  $\text{cm}^{-1}$ ). <sup>c</sup> Tentative assignments are given in parentheses.

als.<sup>27,28</sup> To the contrary, no highly resolved phosphorescence seems to have been reported so far.

We have observed a dramatic change of the fluorescence to phosphorescence intensity ratio upon passing from light to heavy rare gas matrices (Figure 1). Only fluorescence was detected in Ne (Table I), whereas in a Xe matrix the emission is nearly completely dominated by phosphorescence (Table II). Only a trace of fluorescence remains and represents at most 5% of the total emission intensity.

- (18) Bykovskaya, L. A.; Gradyushko, A. T.; Personov, R. I.; Romanovskii, Yu. V.; Solov'ev, K. N.; Starukhin, A. S.; Shul'ga, A. M. *Izv. Akad. Nauk SSSR, Ser. Fiz.* **1980**, *44*, 822.  
 (19) Gladkov, L. L.; Solov'ov, K. N. *Zh. Prikl. Spektrosk.* **1984**, *40*, 275; *Spectrochim. Acta, Part A* **1985**, *41*, 1437.  
 (20) Arabel, S. M.; Shkirman, S. K.; Solov'ov, K. N.; Yegorova, G. D. *Spectrosc. Lett.* **1977**, *10*, 677.  
 (21) Gladkov, L. L.; Gradyushko, A. T.; Solov'ev, K. N.; Starukhin, A. S.; Shul'ga, A. M. *Zh. Prikl. Spektrosk.* **1978**, *29*, 304.  
 (22) Solov'ev, K. N. *Opt. Spectrosc. (Engl. Transl.)* **1961**, *10*, 389.  
 (23) Sevchenko, A. N.; Solov'ev, K. N.; Shkirman, S. F.; Sarzhetskaya, M. V. *Dokl. Akad. Nauk SSSR* **1963**, *153*, 1391.  
 (24) Sevchenko, A. N.; Mashenkov, V. A.; Solov'ev, K. N. *Sov. Phys.—Dokl. (Engl. Transl.)* **1968**, *13*, 213.  
 (25) Sevchenko, A. N.; Solov'ev, K. N.; Mashenkov, V. A.; Shkirman, S. F. *Sov. Phys.—Dokl. (Engl. Transl.)* **1966**, *10*, 778.  
 (26) Solov'ev, K. N.; Gradyushko, A. T.; Tsvirko, M. P. *Izv. Akad. Nauk SSSR* **1972**, *36*, 1107.  
 (27) Bohandy, J.; Kim, B. F. *Spectrochim. Acta, Part A* **1980**, *36*, 463.  
 (28) Kim, B. F.; Bohandy, J. *J. Mol. Spectrosc.* **1978**, *73*, 332.

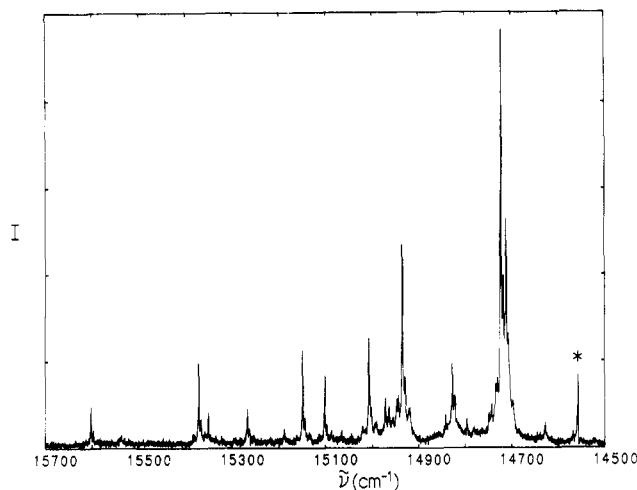


**Figure 2.** Portion of single-site fluorescence of 1- $d_0$  in Ne (4 K, excited at 17 037  $\text{cm}^{-1}$ ). The asterisk marks a peak due to the exciting light, folded around the upper band-pass limit of 15 798  $\text{cm}^{-1}$ .

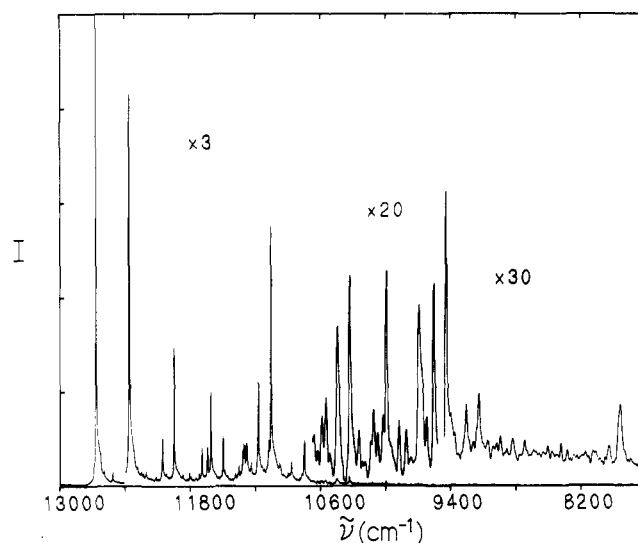


**Figure 3.** Single-site phosphorescence of 1- $d_2$  in Xe (10 K, excited at 16 360  $\text{cm}^{-1}$ ).

Both emissions retain a multiplet structure that we observed previously<sup>11</sup> in the  $S_1 \leftarrow S_0$  absorption spectra. As discussed in more detail below, this site structure is very different for each matrix. Its appearance is particularly interesting for phosphorescence, which usually does not reveal the site pattern observed in absorption or fluorescence.

By carefully choosing the excitation wavelength, we were able to obtain single-site selected fluorescence and phosphorescence spectra (Figures 2 and 3). Such a measurement is quite difficult, due to the photoinduced double-proton-transfer reaction, which leads to a fairly rapid depopulation of the spectrally pumped site and thus to a decrease in signal intensity. This reaction can be slowed down by replacing inner hydrogens by deuterium atoms. Therefore, the best signal-to-noise ratio in a single-site spectrum was obtained for 1- $d_2$ . Still, the sensitivity and speed of the FT instrument enabled us to measure single-site selected spectra even for undeuterated porphine, 1- $d_0$ .

Broad-band excitation and laser excitation into the high-energy region, where the absorptions due to different sites overlap, produce a stationary state in which all sites observed in absorption appear also in luminescence.

Replacement of neon or argon by a heavy atom, xenon, exerts a profound influence on the luminescence pattern: fluorescence practically vanishes, and phosphorescence becomes readily detectable. In order to find out to what degree the various photo-physical parameters are influenced by this heavy-atom effect, we measured singlet and triplet decay times. We find that in Ar matrix at 10 K the fluorescence lifetime of 1- $d_0$  is  $15 \pm 3$  ns,

$\bar{\nu}, \text{cm}^{-1}$										
$1-d_0$		$1-d_2$		$1-d_4$		$1-d_8$		$1-d_{12}$		symmetry
A	B	A	B	A	B	A	B	A	B	
155	156	155	157	155	156	153	153	152	154	$a_g$
308	309	308	307	308	308	303	302	302	302	$a_g$
464	465	462	460	463	464	456	456	454	455	$a_g$
619	618	615	614	612	617	609	604	603	602	$a_g$
				663	663			655	655	$a_g$
722	723	721	722			722	719			$a_g$
						793	793	773	771	
952	956	950	953	972	972	944	944	923	923	$a_g$
		979	978					957	955	
988	991						978			$a_g$
1031	1031	1029	1030	1015	1017					$a_g$
1056	1061	1056	1060							$a_g$
		1062								
				1072	1073					
							1095	1072	1073	
1150	1152							1103	1100	
1176	1177	1175	1176				1171			$a_g$
1221	1223							1228	1228	$b_{1g}$
			1288							
		1316	1317							
				1331	1326					
						1349	1352			
1374	1368	1369	1362	1364	1366			1359	1356	
1388	1391	1385	1388	1384	1385					$b_{1g}$
	1405			1402	1402	1401	1405	1398	1403	
		1428	1428	1422	1422					
								1451	1453	
1497	1496	1496	1495							$a_g$
		1555	1547							
1614	1615	1614	1614	1587	1585	1615	1613	1598	1598	$a_g$
				1601	1602					
				1621	1624					
				1637	1638					
								1664	1665	
1687	1690	1692	1695							
				1710	1712					
			1735							
						1756	1758			
1769	1770	1768	1775							$a_g$
1806	1805	1804	1802							
				1895						
1921	1923	1920	1920	1909	1910	1915	1917	1899	1901	$a_g$
			2004							
								2055	2055	
				2064						
			2078							
			2115							

TABLE II (Continued)

$\bar{\nu}$ , cm <sup>-1</sup>										symmetry
1- <i>d</i> <sub>0</sub>		1- <i>d</i> <sub>2</sub>		1- <i>d</i> <sub>4</sub>		1- <i>d</i> <sub>8</sub>		1- <i>d</i> <sub>12</sub>		
A	B	A	B	A	B	A	B	A	B	
				3023	3023					
		3041								
	3109		3108							
		3158								
				3185	3186					
				3200	3201					
				3218	3222					
3225		3229								a <sub>g</sub>
		3269								
		3307								
					3401					
		3414								
	3465	3491								
					3508					
			3530							
		3725								
		4828								a <sub>g</sub>

<sup>a</sup> Location of origins (cm<sup>-1</sup>, site A, site B): 1-d<sub>0</sub>, 12 677, 12 588; 1-d<sub>2</sub>, 12 673, 12 583; 1-d<sub>4</sub>, 12 705, 12 615; 1-d<sub>8</sub>, 12 688, 12 600; 1-d<sub>12</sub>, 12 704, 12 621.

TABLE III: Triplet Decay Times Measured by Flash Photolysis (10 K)

	decay time, ms	matrix
1-d <sub>0</sub>	0.63 ± 0.07	Xe
	2.6 ± 0.3	Ar
1-d <sub>2</sub>	0.85 ± 0.20	Xe
1-d <sub>4</sub>	0.69 ± 0.07	Xe
1-d <sub>8</sub>	0.73 ± 0.07	Xe
1-d <sub>12</sub>	0.95 ± 0.10	Xe

essentially the same as that reported<sup>9</sup> in *n*-octane at 4 K (17 ± 3 ns). It is known from other work<sup>29</sup> that the intersystem crossing (ISC) quantum yield is 0.90 in toluene, and we may safely assume similar efficiency in Ne and at least as much in Ar. Thus, while the decrease of fluorescence intensity upon going from Ne to Xe is in keeping with the expected enhanced S<sub>1</sub> → T<sub>1</sub> ISC rate, this alone cannot account for the observed large increase in phosphorescence yield. The radiative rate constant of T<sub>1</sub> depopulation must be strongly increased in Xe matrix.

This conclusion is nicely confirmed by comparing triplet-state lifetimes and phosphorescence quantum yields in Ar and Xe (Table III). At 10 K, the triplet state of 1-d<sub>0</sub> decays in 630 μs in Xe and over 4 times more slowly in Ar. While we do not have a quantitative measurement of the emission quantum yield, we estimate that the phosphorescence yields in Ar and Xe differ by a factor of more than 100. One can write

$$\Phi_P = \Phi_{ISC} k_P \tau_T$$

where  $\Phi_P$  and  $\Phi_{ISC}$  are the quantum yields of phosphorescence and S<sub>1</sub> → T<sub>1</sub> intersystem crossing, respectively,  $k_P$  is the radiative rate of T<sub>1</sub> depopulation, and  $\tau_T$  is the triplet decay time. Since the ratio of intersystem crossing efficiencies in Ar and Xe is close to one, we obtain

$$\frac{k_P(\text{Xe})}{k_P(\text{Ar})} \approx \frac{\tau_T(\text{Ar})\Phi_P(\text{Xe})}{\tau_T(\text{Xe})\Phi_P(\text{Ar})}$$

Thus, the radiative rate constant of the triplet state of porphine in Xe increases by more than 2 orders of magnitude with respect to Ar. This huge external heavy-atom effect on the spin-forbidden radiative rate constant may turn out to be common. Recently, a 300-fold increase of the phosphorescence rate constant in Xe with respect to Ar was observed in (dimethylamino)benzonitrile,<sup>30</sup> while the nonradiative rate of triplet depopulation increased less

than 5 times, similarly as in our case.

Triplet decay lifetimes in variously deuterated porphines (Table III) follow the trend reported for different porphyrin free bases in ethanol glasses at 77 K;<sup>31</sup> the lifetimes become longer with increasing degree of deuteration.

Finally, it is probably not accidental that the triplet decay time in 1-d<sub>0</sub> in Xe is close to the value reported<sup>2</sup> for this compound in EPA/EtI glass (about 1 ms). Iodine and xenon are neighbors in the periodic table and thus may cause a similar heavy-atom effect.

**Vibronic Structure of Luminescence.** Tables I and II show the energies and symmetries of ground-state vibrations obtained from the vibronic structure of luminescence. The polarization of the vibronic bands was determined either by a luminescence polarization measurements or by comparison with a corresponding band observed in absorption. Since the symmetry of the latter is known<sup>11</sup> from LD measurements on a photooriented sample, fairly reliable symmetry assignments can be made even for those luminescence transitions that were too weak for polarization determination.

Our data for the fluorescence of 1-d<sub>0</sub> reveal 24 previously known bands, plus many that were not previously observed: 608, 874, 1027, 1103, 1256, 1278, 1301, 1379, 1467, 1480, 1502, 1578, 1657, 1693, 1752, and 1801 cm<sup>-1</sup>; the band at 1575 cm<sup>-1</sup> was reported for porphine in anthracene crystal,<sup>28</sup> but not in Shpol'skii matrices. We did not detect the reported vibronic band corresponding to a 420-cm<sup>-1</sup> vibration, although according to the literature<sup>15</sup> it should be more than an order of magnitude more intense than our detection limit.

In several cases our polarization assignments differ from previous ones. The vibrations at 1134 and 1600 cm<sup>-1</sup> were previously proposed to have a<sub>g</sub> symmetries, and those at 1175 and 1612 cm<sup>-1</sup>, b<sub>1g</sub> symmetries.<sup>15</sup> We find that the former have b<sub>1g</sub> symmetry and the latter a<sub>g</sub> symmetry, in perfect agreement with results of site-selection spectroscopy.<sup>18</sup> A detailed discussion will be given elsewhere.<sup>32</sup>

Here, we focus our attention on phosphorescence, since its vibronic structure has not been previously studied. Broad phosphorescence of 1-d<sub>0</sub> was reported<sup>2</sup> in a 50:50 EPA/ethyl iodide mixture. Extremely weak phosphorescence showing several vibronic bands was observed<sup>3</sup> in a mixture of benzene and isooctane. The position of its 0-0 origin agrees well with our result.

Comparison of the vibronic structures of fluorescence and phosphorescence reveals significant differences between the two

(29) Gradyushko, A. T.; Tsvirko, M. P. *Opt. Spectrosc. (Engl. Transl.)* **1971**, *31*, 291.

(30) Morgan, M. A.; Pimentel, G. C. *J. Phys. Chem.* **1989**, *93*, 3056.

(31) Burgner, R. P.; Ponte Goncalves, A. M. *Chem. Phys. Lett.* **1977**, *46*, 275.

(32) Radziszewski, J. G.; Nepřas, M.; Waluk, J.; Vogel, E.; Michl, J. Unpublished results.

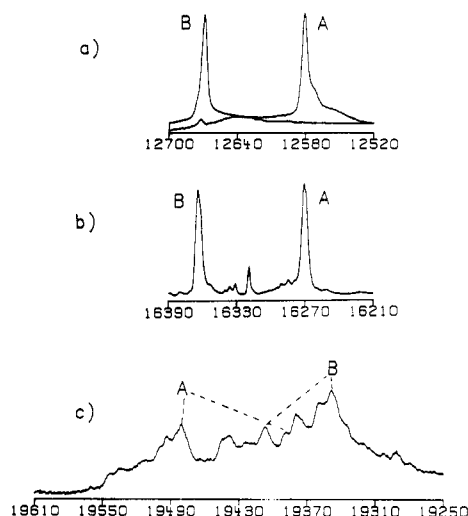


**Figure 4.** Porphine ( $1-d_0$ ) in Xe matrix at 10 K: (a) the 0-0 phosphorescence bands obtained upon exciting into site A (right) and B (left); (b) the 0-0 absorption region of the  $S_1(Q_x)$  state; (c) the 0-0 absorption region of the  $S_2(Q_y)$  state. (Sites A and B are both split into subsites as indicated by dashed lines.)

emissions. In fluorescence, the intensity of bands corresponding to non-totally symmetric vibrations ( $b_{1g}$ ) is enhanced with respect to bands corresponding to totally symmetric vibrations ( $a_g$ ). This is because the latter are much weaker than in absorption; the phenomenon has already been noticed in Shpolskii matrices.<sup>15</sup> In phosphorescence, on the contrary, mostly totally symmetric vibrations are active, with the 0-0 band particularly strong, while the bands corresponding to  $b_{1g}$  transitions are very strongly suppressed or not observed at all. This is most likely related to the external heavy atom induced origin of the phosphorescence, since the 0-0 peak is very weak in the phosphorescence spectrum reported<sup>3</sup> in an isoctane/benzene mixture.

The other difference between the two emissions concerns progressions of the vibronic bands. While fluorescence is "typical" for porphyrins in that no strong progressions are observed, phosphorescence reveals a nice progression based on a  $1614\text{-cm}^{-1}$  mode. We were quite surprised to detect even the second overtone of this vibration in  $1-d_2$ , where it lies  $4828\text{ cm}^{-1}$  to the red of the origin, i.e., at  $7842\text{ cm}^{-1}$ !

**Site Structure.** The fluorescence of  $1-d_0$  in Ne reveals the same site pattern as in  $S_1 \leftarrow S_0$  absorption: two main groups of sites are observed, A and B, each consisting of at least three components (subsites). Additional lower intensity sites are also observed in both absorption and emission. The relative intensities of the fluorescence lines corresponding to different multiplets as well as of those within a multiplet strongly depend on the excitation wavelength. We used this observation to determine whether a particular line belongs to a separate vibronic transition or to another site of the same vibronic band. This turned out to be useful in the spectrally congested region commencing about  $1000\text{ cm}^{-1}$  to the red of the fluorescence origin. This procedure enabled us to detect more transitions than observed in single-site selected spectra, since the latter had to be recorded quite rapidly, due to intensity decrease resulting from phototautomerization.

We have previously reported<sup>11</sup> that the absorption site pattern for the  $S_2(Q_y)$  transition is completely different from that of  $S_1(Q_x)$ : the energy separation becomes larger, the dominant sites split into several components, and the energy ordering of the A and B sites is reversed with respect to that in  $S_1$ . The site pattern of phosphorescence perfectly matches that observed in the  $S_1(Q_x) \leftarrow S_0$  absorption (Figure 4). It consists of two main sites, A at lower and B at higher energy. These sites are separated by  $89\text{ cm}^{-1}$  in emission and  $93\text{ cm}^{-1}$  in absorption. A weaker site, X, lying between A and B in  $Q_x \leftarrow S_0$  absorption, is also detected in phosphorescence.

The finding that phosphorescence retains the site pattern observed in absorption is rather unexpected and, to our knowledge, has not been frequently reported. Perhaps even more interesting

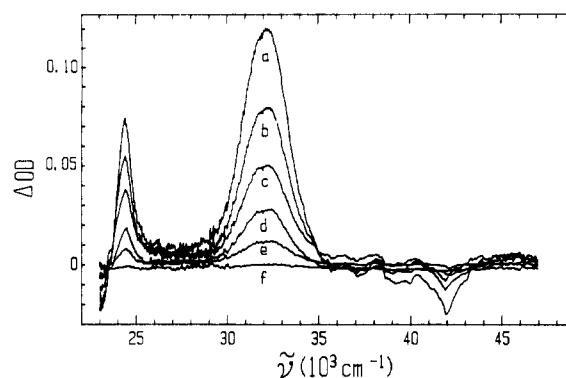


**Figure 5.** T-T absorption curves of  $1-d_0$  in Ar (10 K), obtained after the following delays between the pump and probe pulses: (a)  $10\text{ }\mu\text{s}$ , (b)  $900\text{ }\mu\text{s}$ , (c)  $2\text{ ms}$ , (d)  $4\text{ ms}$ , (e)  $8\text{ ms}$ , and (f)  $16\text{ ms}$ .

is the fact that a comparison of site structure patterns observed in both fluorescence and phosphorescence with the shapes of  $S_1(Q_x) \leftarrow S_0$  and  $S_2(Q_y) \leftarrow S_0$  absorption bands, characteristic and very different from each other, makes it very clear that the phosphorescence site pattern corresponds to that observed in  $S_1 \leftarrow S_0$  as opposed to  $S_2 \leftarrow S_0$  absorption. It is particularly noteworthy that the energy order of the sites in phosphorescence, A below B, is the same as in  $S_1 \leftarrow S_0$  absorption, while it is the opposite in  $S_2 \leftarrow S_0$  absorption. A likely implication is that the orbital origins of the lowest singlet and triplet states are the same.

This, however, disagrees with the presently accepted assignment of the lowest triplet state as  $Q_y$ , proposed on the basis of comparison of ESR results in *n*-octane crystal with PPP calculations.<sup>4</sup> The two lowest singlet states of porphine,  $S_1(Q_x, B_{3u})$  and  $S_2(Q_y, B_{2u})$ , are separated by only about  $3000\text{ cm}^{-1}$ . The two corresponding triplet transitions presumably lie even closer to each other.<sup>33</sup> Our results suggest quite strongly that, at least in Xe, the phosphorescence of porphine occurs from the  $Q_x$  triplet state.

**Triplet-Triplet Absorption.** Figure 5 presents the T-T absorption spectra of  $1-d_0$  in Ar matrix. The spectra in Xe are virtually identical. Two strong bands are observed, one on the low-energy side of the Soret bands and the other on the high-energy side. The former band has been previously reported,<sup>34,35</sup> whereas we did not find a literature reference to the other transition, with a maximum around  $310\text{ nm}$ . According to PPP calculations,<sup>34</sup> numerous allowed T-T transitions are to be expected in the near-UV and blue visible regions.

Comparison of the intensities of the T-T absorption bands with the intensity of the bleached  $Q_x$  and  $Q_y$  bands shows that the two observed  $T_n \leftarrow T_1$  transitions are quite intense, about 5 times stronger than the  $Q_y$  band. However, they are weaker than the Soret bands. This may be seen from Figure 5, where the intensity of Soret transitions is so high that practically no light passes through the sample in this spectral region, making it impossible to detect absorbance changes.

Additional T-T bands are observed above  $600\text{ nm}$ , in agreement with previous results.<sup>34</sup> The sensitivity of our spectrometer in this region was insufficient to permit a quantitative analysis.

**Photoinduced Double Proton Transfer.** Since the pioneering studies of Weller describing excited-state proton transfer in  $\alpha$ -naphthol<sup>36</sup> and methyl salicylate,<sup>37</sup> many compounds were found to exhibit this type of reaction. Photoinduced shift of the two inner protons in porphine was discovered more than 15 years ago,<sup>5-8</sup>

(33) Weiss, C.; Kobayashi, H.; Gouterman, M. *J. Mol. Spectrosc.* **1965**, *16*, 415. Knoop, J. V.; Knop, A. *Z. Naturforsch., A: Phys., Phys. Chem., Kosmophys.* **1970**, *25*, 1720. Sundbom, M. *Acta Chem. Scand.* **1968**, *22*, 1317.

(34) Sapunov, V. V.; Solov'ev, K. N.; Tsvirko, M. P. *Zh. Prikl. Spektrosk.* **1974**, *21*, 667.

(35) Reddi, E.; Jori, J. *Rev. Chem. Intermed.* **1988**, *10*, 241.

(36) Weller, A. *Z. Elektrochem.* **1952**, *56*, 662; *Z. Phys. Chem.* **1958**, *17*, 224.

(37) Weller, A. *Naturwissenschaften* **1955**, *42*, 175; *Z. Elektrochem.* **1956**, *60*, 1144; *Prog. React. Kinet.* **1961**, *1*, 189.

but the mechanism of the process is still not clearly understood. It has been speculated<sup>8</sup> that the reaction may be associated with vibrational relaxation that follows the intersystem crossing from  $S_1$  to the triplet manifold or from  $T_1$  into the vibrationally excited levels of the ground state. Tunneling between the vibrationless levels of the two tautomeric forms in the lowest excited singlet state was excluded, and the same conclusion had been reached earlier for the first triplet state.<sup>38</sup>

Another model proposed for the photoreaction observed in several porphine derivatives<sup>39</sup> assumes the transient formation of a "cis" tautomer (**2**), in which protons are located on adjacent nitrogen atoms. The energy of such a structure was postulated to be lower than that of a "normal" trans form in the  $T_1$  state and higher in the  $S_0$  state. Quite recently, the existence of a cis tautomer in the ground state was suggested by NMR.<sup>40</sup> Other hypothetical forms have also been proposed.<sup>41</sup>

We now summarize those observations made in rare gas matrices that promise to shed some light onto the mechanism of the reaction.

(i) The yields of photoinduced proton transfer from site A to B and from site B to A are the same within experimental error (10%). The relative efficiencies were measured by first transferring the population from one site into the other by laser irradiation and then monitoring changes in the visible absorption spectrum while simultaneously irradiating both sites. The latter was achieved by using the light source of the FT spectrophotometer, which simultaneously was recording the absorption.

(ii) We observed an isotope effect on the proton-transfer efficiency in  $1-d_2$  vs  $1-d_0$ . The photoinduced reaction was roughly an order of magnitude slower in the deuterated compound.

(iii) The tautomerization yield in Xe and Kr matrices was practically temperature independent in the range 10–40 K. At higher temperatures, the reaction yield increased considerably.

(iv) Photoinduced double proton transfer is slower in the heavier inert gas matrices. This was found upon observing how long the sample photooriented by irradiation with polarized light remained dichroic while being exposed to the analyzing light of the instrument. The LD signal decreased much faster in Ar than in

Xe matrices. It should be noted that, at the temperatures used, the rate of the dark ground-state reaction is completely negligible.

(v) Single-site fluorescence and phosphorescence spectra were obtained from both dominant sites, A and B.

The fact that single-site emissions are observed is difficult to reconcile with a model of reaction occurring on the excited-state energy surface with only two minima, since in this case one would expect to see emissions from both sites even after selective excitation of only one site, unless the efficiency of the process is very weak. On similar grounds, "hot" triplet state reaction also seems improbable.

Although our results clearly cannot be said to "prove" any mechanism, they are perfectly compatible with a model of tautomerization occurring in the lowest triplet state and involving a third, lower energy minimum, most probably corresponding to the cis tautomeric structure (**2**).<sup>39</sup> The molecule would move into this minimum in a rate-determining step by proton tunneling and at higher temperatures also by barrier crossing; see (iii) above. Fast intersystem crossing to the ground state of the cis form would then occur, promoted by the presumably lower  $T_1$ – $S_0$  gap in **2**, followed by return to the trans species of either the substrate or product. In this model, the efficiency of the tautomerization process should be directly proportional to the triplet lifetime, and thus higher in the lighter inert gas matrices, exactly as observed.

A definitive proof of such a scheme would be the direct observation of the cis triplet intermediate **2** in absorption or emission. The difficulty is that such a species is most probably extremely short-lived. Its presence might well be obscured in absorption by much higher populations of the triplet state of the usual trans isomer **1**. The phosphorescence quantum yield of the cis form might well be very small and the wavelength very inconvenient for sensitive detection.

The above observation (iii) provides a hint against the hot  $S_0$  state mechanism, since the rate of vibrational cooling of a hot porphine molecule in the matrix should not be temperature-independent.

We are currently continuing our mechanistic investigation; preliminary results indicate that direct irradiation into the origin of the  $T_1 \leftarrow S_0$  transition to the lowest triplet state of site A produces a slow change in the relative site population. By avoiding the  $S_1$  state, this would prove that the tautomerization is capable of proceeding on the  $T_1$  or the  $S_0$  surface.

**Acknowledgment.** This work was supported by grants from the National Science Foundation (CHE9000292) and the National Institutes of Health (GM 37929).

(38) Van Dorp, W. G.; Schoemaker, W. M.; Soma, M.; van der Waals, J. H. *Mol. Phys.* **1975**, *30*, 1701.

(39) Dvornikov, S. S.; Kuz'mitskii, V. A.; Knyukshto, V. N.; Solov'ev, K. N. *Dokl. Akad. Nauk SSSR* **1985**, *282*, 362.

(40) Schlabach, M.; Rumpel, H.; Limbach, H.-H. *Angew. Chem., Int. Ed. Engl.* **1989**, *28*, 76.

(41) Bersuker, G. I.; Polinger, V. Z. *Chem. Phys.* **1984**, *86*, 57.

## Scanning Tunneling Microscopy and Tunneling Spectroscopy of n-Type Iron Pyrite (n-FeS<sub>2</sub>) Single Crystals

Fu-Ren Fan and Allen J. Bard\*

Department of Chemistry, The University of Texas at Austin, Austin, Texas 78712 (Received: June 15, 1990; In Final Form: August 21, 1990)

The (001) surface of a highly doped ( $>2.7 \times 10^{18} \text{ cm}^{-3}$ ) n-type FeS<sub>2</sub> crystal was imaged by the constant current mode in air with a scanning tunneling microscope (STM). Current ( $i$ ) images at different bias voltages ( $V$ ) were also obtained. Tunneling spectroscopy (TS) was carried out, and  $i$  vs  $V$  and  $di/dV$  vs  $V$  curves obtained with the tip held above the FeS<sub>2</sub> surface were interpreted in terms of the band locations and a localized state within the band gap. The effect of band bending in the semiconductor on the interpretation of the TS results is also considered.

### Introduction

In this paper we present the results of scanning tunneling microscopy (STM) and related tunneling spectroscopy (TS) and scanning tunneling spectroscopy (STS) studies on the transition-metal dichalcogenide n-FeS<sub>2</sub>. Transition-metal di-

chalcogenides have been shown to be promising semiconductors for electrochemical regenerative and photoelectrolysis cells.<sup>1</sup> Its stability against anodic photocorrosion has been attributed to

(1) Tributsch, H. *Struct. Bonding* **1982**, *49*, 127.